Zinc oxide nanocomb biosensor for glucose detection

Wang, J. X.; Sun, Xiaowei; Wei, A.; Lei, Y.; Cai, X. P.; Li, Chang Ming; Dong, Zhili

2006

Wang, J. X., Sun, X., Wei, A., Lei, Y., Cai, X. P., Li, C. M., et al. (2006). ZnO oxide nanocomb biosensor for glucose detection. Applied Physics Letters, 88(23).

https://hdl.handle.net/10356/99445

https://doi.org/10.1063/1.2210078

Zinc oxide nanocomb biosensor for glucose detection

J. X. Wang, X. W. Sun,[a] and A. Wei
School of Electrical and Electronic Engineering, Nanyang Technological University, Nanyang Avenue, Singapore 639798, Singapore

Y. Lei, X. P. Cai, and C. M. Li
School of Chemical and Biomedical Engineering, Nanyang Technological University, Nanyang Avenue, Singapore 639798, Singapore

Z. L. Dong
School of Materials Science and Engineering, Nanyang Technological University, Nanyang Avenue, Singapore 639798, Singapore

(Received 5 December 2005; accepted 12 April 2006; published online 6 June 2006)

Single crystal zinc oxide nanocombs were synthesized in bulk quantity by vapor phase transport. A glucose biosensor was constructed using these nanocombs as supporting materials for glucose oxidase (GO_x) loading. The zinc oxide nanocomb glucose biosensor showed a high sensitivity (15.33 $\mu A/cm^2$ mM) for glucose detection and high affinity of GO_x to glucose (the apparent Michaelis-Menten constant $K_M^{app}=2.19$ mM). The detection limit measured was 0.02 mM. These results demonstrate that zinc oxide nanostructures have potential applications in biosensors. © *2006 American Institute of Physics*. [DOI: 10.1063/1.2210078]

Zinc oxide (ZnO) is an important member in II-VI group semiconductors. It has profound applications in optics, optoelectronics, sensors, and actuators due to its semiconducting, piezoelectric, and pyroelectric properties.[1,2] One-dimensional (1D) zinc oxide nanostructures have attracted great interest in the past few years.[3,4] Extensive efforts have been made to synthesize ZnO nanostructures, such as nanowires,[3] nanobelts,[5] nanotubes,[6] nanorings,[7] etc., because nanostructural morphology is one of the important factors determining the properties. Recently, ZnO nanodevices, such as room temperature laser,[8] gas sensor,[9] transistor,[10] and field emitter,[11] have been studied extensively. These devices show higher performance compared to those fabricated from bulk and thin film forms of ZnO. On the other hand, ZnO is a biocompatible material with a high isoelectric point (IEP) of about 9.5, which make it suitable for absorption of proteins with low IEPs, as the protein immobilization is primarily driven by electrostatic interaction.[12,13] Moreover, ZnO nanostructures have unique advantages including the high specific surface area, nontoxicity, chemical stability, electrochemical activity, and high electron communication features. Hence, they are promising for biosensor applications. However, biosensors made of 1D ZnO nanostructures are rare.[12]

In this letter, we shall report a biosensor for glucose detection using ZnO nanocombs fabricated in large quantity using a vapor phase transport method. The enzyme used for glucose detection, glucose oxidase (GO_x), was immobilized on ZnO nanocombs first in our design. The immobilized GO_x shows high affinity for glucose, and the ZnO nanocomb biosensor showed high sensitivity without the presence of an electron mediator.

The ZnO nanocombs were prepared by a vapor phase transport method. Firstly, high purity ZnO (99.99%) and graphite powder were mixed thoroughly and loaded into a small quartz boat. Then the small quartz boat was pushed into a large quartz tube mounted horizontally inside a furnace. A slice of silicon wafer was placed downstream from the quartz boat as the collector. The quartz tube was then heated to 900 °C and kept for 30 min. Graphite powder was used to reduce ZnO at this temperature so as to generate Zn and ZnO_x ($x<1$) vapor. At the same time, argon and oxygen were introduced through the tube at a flow rate of 100 (SCCM denotes cubic centimeter per minute at STP) and 1 SCCM, respectively. The pressure of the tube was maintained at about 8×10^{-1} Torr by a rotary pump. After the reaction was terminated, the furnace was cooled down to room temperature and the white products on silicon substrate were collected for characterization and fabrication of glucose sensor. Scanning electron microscopy (SEM, Hitachi S-5200), x-ray diffraction (XRD, Siemens D5005) with Cu $K\alpha$ radiation, high-resolution transmission electron microscopy (HRTEM, JEM-2010F), and selected area electron diffraction (SAED) were employed in characterization.

To fabricate the glucose biosensor, the as-prepared ZnO nanocombs were firstly transferred from the silicon substrate to a standard gold electrode commonly used in electrochemistry. The as-prepared ZnO/Gold electrode was then wetted by 0.01*M* phosphate buffer solution (PBS) with *p*H=7.4, and dried by high purity nitrogen gas. A 5 μl GO_x (~40 U/mg) solution was dropped onto the surface of the ZnO/Gold electrode. The GO_x solution was prepared by dissolving 5.0 mg GO_x in 1.0 ml, 0.01*M* PBS. Following the evaporation of water, subsequently, a 5 μl 0.5% (weight) Nafion solution was dropped onto the GO_x/ZnO/gold electrode and dried overnight at 4 °C to form a film, which is critical to attach GO_x/ZnO nanocombs tightly on the surface of the gold electrode. The Nafion/GO_x/ZnO/gold electrodes were stored in PBS and kept at 4 °C in a refrigerator when not in use. The electrochemical experiment was performed at room temperature utilizing an electrochemical workstation (Bio-logic SA VMP2) with a conventional three-electrode configuration. The modified gold electrode with a diameter of 1 mm was used as the working electrode. Prior to the experiment, the electrode was polished with 1.0, 0.3, and

[a]Author to whom correspondence should be addressed; electronic mail: exwsun@ntu.edu.sg

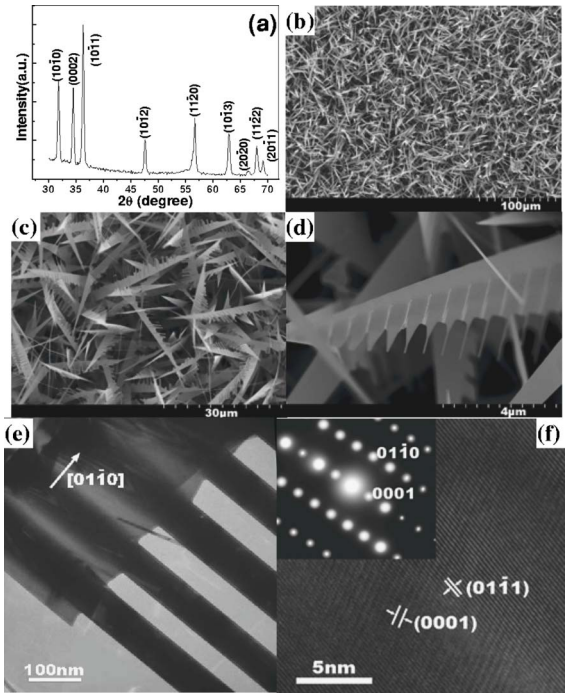

FIG. 1. (a) XRD pattern of ZnO nanocombs and SEM images of ZnO nanocombs with (b) low, (c) medium, and (d) high magnifications, respectively. (e) TEM image of a ZnO nanocomb and (f) HRTEM image and the corresponding SAED pattern (insert) of a ZnO nanocomb.

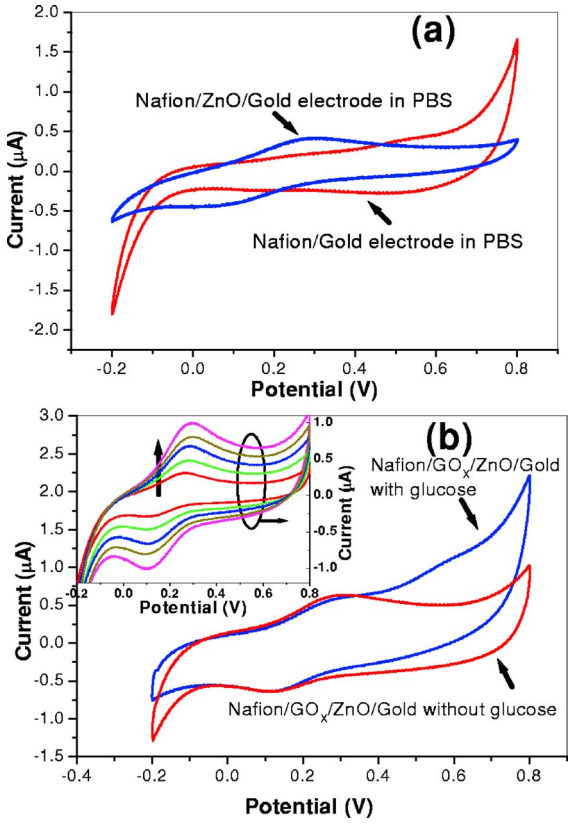

FIG. 2. (Color online) (a) Cyclic voltammograms of Nafion/gold electrode (red) and Nafion/ZnO/gold electrode (blue) in 0.01*M*, *p*H 7.4 PBS buffer at scan rate of 50 mV/s. (b) Cyclic voltammograms of Nafion/GO_x/ZnO/gold electrode in the same buffer solution in the absence (red) and presence (blue) of 3 mM glucose. Inset is the CV curves recorded at various scan rates of 20, 40, 60, 80, and 100 mV/s (sequentially increasing along the arrow direction) of Nafion/GO_x/ZnO/gold electrode in the same buffer solution containing 3 mM glucose.

0.05 μm aluminum slurries sequentially, and then sonicated in de-ionized water.

The XRD pattern of the as-prepared product by vapor phase transport is shown in Fig. 1(a), where all the diffraction peaks can be indexed to the hexagonal wurtzite phase of ZnO with lattice constants of $a=0.325$ nm and $c=0.520$ nm, which match well the standard XRD data file (JCPDS 79-2205). No other crystalline forms, such as Zn or other Zn compounds, were detected.

Figures 1(b)–1(d) show typical SEM images of the ZnO product in low, medium, and high magnifications, respectively. It can be seen that the product consists of numerous comblike nanostructures with single morphology (nanocomb) and uniform size in the area examined. Unlike the nanocombs reported previously,[14] the stems of nanocombs are ribbons with a thickness of about 50 nm, the length of the main stems reaches several tens of micrometers, and the width of the stems decreases gradually along the growth direction to form sharp tips. The branching nanorods grow on one side of nanoribbon with a diameter of about 200 nm. The distance between two adjacent nanorods is about 500 nm.

The detailed structure of individual ZnO nanocomb is studied by SAED and TEM. Figure 1(e) shows the TEM image of an individual ZnO nanocomb. The ribbon stem and the nanorods of ZnO nanocomb show different contrast, indicating different thicknesses for the stem and the nanorods. Figure 1(f) is a HRTEM image taken near the edge along the stem of the nanocomb in Fig. 1(e). The spacing of the lattice planes, 0.520 and 0.246 nm, corresponds to the interspacing of (0001) and (01$\bar{1}$1) planes of wurtzite ZnO, respectively. The HRTEM image confirms the good quality of the single crystal ZnO nanocombs. The corresponding SAED pattern is shown in the inset in Fig. 1(f). The growth direction of the stem and branching nanorods can be determined to be [01$\bar{1}$0] and [0001], respectively. The direction of electron beam, which is vertical to the ribbon stem of the nanocomb, is indexed to be [2$\bar{1}\bar{1}$0]

The performance of the GO_x/ZnO biosensor was measured at room temperature. Cyclic voltammograms (CV) of Nafion/gold electrode and Nafion/ZnO/gold electrode are shown in Fig. 2(a). Different from pure Nafion/gold electrode, two peaks at 0.3 and 0.1 V were observed in the CV curve of Nafion/ZnO/gold electrode. These two peaks should be related to oxidation and reduction of ZnO itself. The origin of these two peaks will be studied in detail in a separate paper. Figure 2(b) shows the CV curves of Nafion/GO_x/ZnO/gold electrode in PBS with 0 and 3 mM glucose, respectively. It can be seen that there is an increase in current from 0.4 to 0.6 V in PBS with 3 mM glucose compared to PBS without glucose, indicating the response of Nafion/GO_x/ZnO/gold electrode to glucose. A weak shoulder peak appeared at about 0.6 V on the CV curve for Nafion/GO_x/ZnO/gold electrode in PBS with 3 mM glucose. This peak can be attributed to H_2O_2 generated during glucose oxidation by GO_x, as reported previously.[15,16] The inset shows the CV curves of Nafion/GO_x/ZnO/gold electrode in PBS containing 3 mM glucose obtained at various scan rates of 20, 40, 60, 80, and 100 mV s^{-1} (sequentially increase along the arrow direction in the inset), respectively. It can be found that the peak current is proportional to the square root of scan rate, showing a typical diffusion-controlled electrochemical behavior.

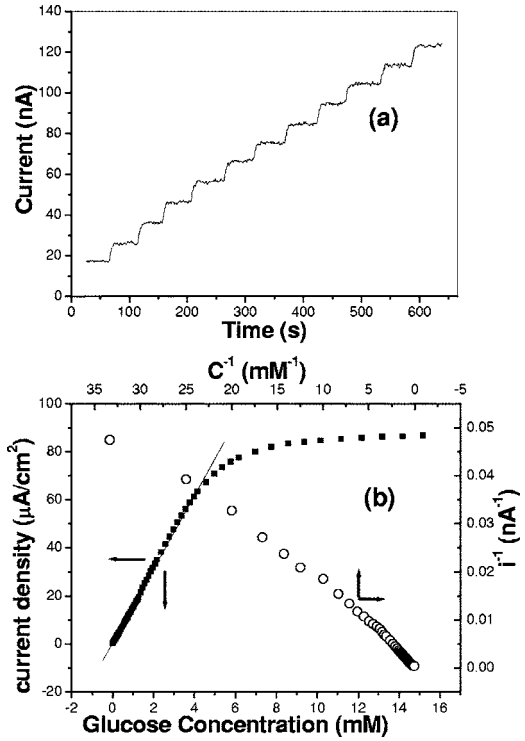

FIG. 3. (a) Amperometric responses of Nafion/GO_x/ZnO/gold electrodes with the successive addition of 20 μM glucose to the 0.01*M*, *p*H 7.4 PBS buffer under stirring. (b) The calibration curve (solid square) of ZnO/GO_x biosensor and the Lineweaver-Burk plot (open circle). The straight line is the linear fit to the calibration curve. A potential of +0.8 V (vs Ag/AgCl reference) was applied on the working electrode in the measurement.

Figure 3(a) displays a typical amperometric response of the ZnO biosensor after addition of successive aliquots of 20 μM glucose in PBS under stirring. It can be seen from the plot that the biosensor shows a rapid and sensitive response to the change of glucose concentration, indicating a good electrocatalytic property of Nafion/GO_x/ZnO/gold electrode. The response time for the electrode is less than 10 s. The corresponding calibration curve (solid square) of the glucose biosensor is shown in Fig. 3(b). Following the increase of the glucose concentration, the response current increases and saturates at a high glucose concentration of 13 mM. The linear range of the calibration curve is from 0.02 to 4.5 mM (correction coefficient $R=0.999$) with a sensitivity of 15.33 $\mu A/cm^2$ mM and a limit of detection (LOD) of 0.02 mM. The sensitivity is significantly higher than that of glucose biosensor reported previously,[17,18] and the LOD is lower compared to the glucose sensor based on titanium dioxide sol-gel matrix reported previously.[19] The apparent Michaelis-Menten constant K_M^{app} is generally used to evaluate the biological activity of immobilized enzyme. It could be calculated according to the Lineweaver-Burk equation $1/i=(K_M^{app}/i_{max})(1/C)+1/i_{max}$, where i is the current, i_{max} is the maximum current, and C is the glucose concentration. The Lineweaver-Burk plot (open circle) of $1/i$ vs $1/C$ is shown in Fig. 3(b). According to the Lineweaver-Burk plot, the K_M^{app} is calculated to be 2.19 mM, which is lower than previously reported data using native enzyme GO_x,[20] Au nanoparticle,[21] and nanopore-TiO_2 film electrodes,[20,22] indicating the high affinity of the ZnO glucose biosensor.

Metal oxides have unique advantages in immobilized enzyme. Different enzymes immobilized on the porous metal oxide matrix have been reported.[22–24] In our case, the ZnO nanocombs are distributed irregularly on the surface of the gold electrode forming a three-dimensional porous network. Meanwhile, the ZnO nanocombs with ribbonlike stem possess high specific surface area and good biocompatible properties, which provides a favorable microenvironment for GO_x loading with large quantity. Additionally, at working buffer *p*H, ZnO nanocombs are positively charged whereas GO_x is negatively charged, which favors the electrostatic attraction of GO_x and ZnO nanocombs. Moreover, as a traditional transparent conductor, single crystalline ZnO nanostructures have good conductivity, which provide many transport channels in nanoscale, thus enhancing the direct electron transfer between the active sites of enzyme and the electrode. These reasons contribute to the high sensitivity and high affinity of the biosensor constructed by ZnO nanocombs.

In summary, we reported a biosensor by immobilized GO_x on the single crystalline ZnO nanocombs for glucose detection. The results showed that the ZnO nanocombs formed an attractive matrix for GO_x immobilization, which exhibits a high affinity, high sensitivity, and fast response for glucose detection. This simple method of fabricating ZnO/GO_x biosensor can also be extended to immobilize other enzymes and other bioactive molecules on various 1D metal oxide nanostructures, and form versatile electrodes for biosensor studies.

The sponsorships from Research Grant Manpower Fund (RGM 21/04) of Nanyang Technological University and Science and Engineering Research Council grant (0421010010) from Agency for Science, Technology and Research (A*STAR), Singapore, are gratefully acknowledged.

[1] D. P. Norton, Y. W. Heo, M. P. Ivill, S. J. Pearton, M. F. Chisholm, and T. Steiner, Mater. Today **7**, 34 (2004).
[2] X. W. Sun and H. S. Kwok, J. Appl. Phys. **86**, 408 (1999).
[3] Y. Li, G. W. Meng, L. D. Zhang, and F. Phillipp, Appl. Phys. Lett. **76**, 2011 (2000).
[4] C. X. Xu, X. W. Sun, Z. L. Dong, and M. B. Yu, Appl. Phys. Lett. **85**, 3878 (2004).
[5] Z. W. Pan, Z. R. Dai, and Z. L. Wang, Science **291**, 1947 (2001).
[6] W. Z. Xu, Z. Z. Ye, D. W. Ma, H. M. Lu, L. P. Zhao, B. H. Zhao, X. D. Yang, and Z. Y. Xu, Appl. Phys. Lett. **87**, 093110 (2005).
[7] P. M. Gao, Y. Ding, W. J. Mai, W. L. Hughes, C. S. Lao, and Z. L. Wang, Science **309**, 1700 (2005).
[8] X. W. Sun, S. F. Yu, C. X. Xu, C. Yuen, B. J. Chen, and S. Li, Jpn. J. Appl. Phys., Part 2 **42**, L1229 (2003).
[9] Z. Y. Fan and J. G. Lu, J. Nanosci. Nanotechnol. **5**, 1561 (2005).
[10] Z. Y. Fan and J. G. Lu, Appl. Phys. Lett. **86**, 123510 (2005).
[11] C. X. Xu and X. W. Sun, Appl. Phys. Lett. **83**, 3806 (2003).
[12] F. F. Zhang, X. L. Wang, S. Y. Ai, Z. D. Sun, Q. Wan, Z. Q. Zhu, Y. Z. Xian, L. T. Jin, and K. Yamamoto, Anal. Chim. Acta **519**, 155 (2004).
[13] Z. M. Liu, Y. L. Liu, H. F. Yang, Y. Yang, G. L. Shen, and R. Q. Yu, Electroanalysis **17**, 1065 (2005).
[14] Z. L. Wang, X. Y. Kong, and J. M. Zuo, Phys. Rev. Lett. **91**, 185502 (2003).
[15] X. Chen and S. J. Dong, Biosens. Bioelectron. **18**, 999 (2003).
[16] Y. H. Yang, H. F. Yang, M. H. Yang, Y. L. Liu, G. L. Shen, and R. Q. Yu, Anal. Chim. Acta **525**, 213 (2004).
[17] T. J. Chara, R. Rajagopalan, and A. Heller, Anal. Chem. **66**, 2451 (1994).
[18] J. C. Vidal, E. Garcia, and J. R. Castillo, Biosens. Bioelectron. **13**, 67 (1998).
[19] J. H. Yu, S. Q. Liu, and H. G. Ju, Biosens. Bioelectron. **19**, 401 (2003).
[20] R. A. Kamln and G. S. Wilson, Anal. Chem. **52**, 1196 (1980).
[21] S. X. Zhang, N. Wang, H. J. Yu, Y. M. Niu, and C. Q. Sun, Bioelectrochemistry **67**, 15 (2005).
[22] Q. W. Li, G. A. Luo, J. Feng, Q. Zhou, L. Zhang, and Y. F. Zhu, Electroanalysis **13**, 413 (2001).
[23] Y. Zhang, P. L. He, and N. F. Hu. Electrochim. Acta **49**, 1981 (2004).
[24] Z. J. Liu, B. H. Liu, J. L. Kong, and J. Q. Deng, Anal. Chem. **72**, 4707 (2000).